Generic topological criterion for flat bands in two dimensions

Alireza Parhizkar 1 and Victor Galitski 1,2

¹Joint Quantum Institute, University of Maryland, College Park, Maryland 20742, USA ²Center for Computational Quantum Physics, The Flatiron Institute, New York, New York 10010, USA



(Received 12 January 2023; revised 29 August 2024; accepted 3 September 2024; published 13 September 2024)

We show that the continuum limit of moiré graphene is described by a (2+1)-dimensional field theory of Dirac fermions coupled to two classical vector fields: a periodic gauge and a spin field. We further show that the existence of a flat band implies an effective dimensional reduction, where the time dimension is "removed." The resulting two-dimensional Euclidean theory contains the chiral anomaly. The associated Atiyah-Singer index theorem provides a self-consistency condition for flat bands. In the Abelian limit, where the spin field is disregarded, we reproduce a periodic series of quantized magic angles known to exist in twisted bilayer graphene in the chiral limit. However, the results are not exact. If the Abelian field has zero total flux, perfectly flat bands can not exist, because of the leakage of edge states into neighboring triangular patches with opposite field orientations. We demonstrate that the non-Abelian spin component can correct this and completely flatten the bands via an effective renormalization of the Abelian component into a configuration with a nonzero total flux. We present the Abelianization of the theory where the Abelianized flat band can be mapped to that of the lowest Landau level. We show that the Abelianization corrects the values of the magic angles consistent with numerical results. We also use this criterion to prove that an external magnetic field splits the series into pairs of magnetic field-dependent magic angles associated with flat moiré-Landau bands. The topological criterion and the Abelianization procedure provide a generic practical method for finding flat bands in a variety of material systems including but not limited to moiré bilayers.

DOI: 10.1103/PhysRevB.110.L121111

Moiré phenomena in twisted bilayer graphene [1–11] and other systems [12,13] have been an active topic of research in recent years. Of particular interest for the former are flat bands, where localized electrons exhibit a variety of strongly correlated phases. In this Letter, we draw a universal picture for the occurrence of the flat bands through emergent gauge fields and the anomaly.

Consider a bilayer graphene system with a small twist and/or strain applied to the layers. As emphasized in Ref. [12], both can be described in terms of a diffeomorphism: $\xi_{\omega} \equiv$ $\epsilon \omega(\mathbf{r})\mathbf{r}$ for strain and $\boldsymbol{\xi}_{\theta} \equiv \epsilon \theta(\mathbf{r})\hat{z} \times \mathbf{r}$ for a twist (parameterized by $\epsilon \ll 1$). With ξ_{ω} and ξ_{θ} being orthogonal to each other and thus forming a basis, all possible flows in two dimensions can be described as a linear combination of these two fields. Therefore a bilayer system with a general infinitesimal deformation can be achieved by applying the diffeomorphism ${f r}
ightarrow {f r} + {m \xi}_{\omega, heta}/2$ to one layer and ${f r}
ightarrow {f r} - {m \xi}_{\omega, heta}/2$ to the other, as in Fig. 1. A finite deformation is reached by successively applying such diffeomorphisms. The time dependent moiré fields $\omega(t, \mathbf{r})$ and $\theta(t, \mathbf{r})$ can be further looked at as bosonic phononlike degrees of freedom for the bilayer system.

Focusing on only one valley, K, in the Brillouin zone, an electron that hops from the K point of one layer to that of the other, can do so along three different momentum vectors that will form the moiré reciprocal lattice vectors of the bilayer system. This is because the deformation has separated the equivalent K points in three different ways (along $\mathbf{q}_{1,2,3}^{\theta}$ for twist and $\mathbf{q}_{1,2,3}^{\omega}$ for strain as depicted in Fig. 1) that are related to each other by a $2\pi/3$ rotation. For the general deformation, these vectors are given by $\mathbf{q_1} \equiv 2K_D(\sinh\frac{\omega}{2}\hat{x} - \sin\frac{\theta}{2}\hat{y})$ with $\mathbf{q}_{2,3}$ derived by successive $2\pi/3$ rotations of \mathbf{q}_1 , while K_D is the distance between K-points of the undeformed Brillouin zone and its center.

The moiré lattice constant, L, can be read off of the magnitude of the moiré reciprocal lattice vectors, $|\mathbf{q}| = 2K_D(\sinh^2\frac{\omega}{2} + \sin^2\frac{\theta}{2})^{1/2}$, which is equal to the distance between the corresponding K points (denoted by k and k' in Fig. 1): $L = 4\pi/3|\mathbf{q}|$. If the electron hops from one layer to the other without changing its position, it acquires a phase determined only by the moiré reciprocal lattice vectors. The dynamics of this electron is given by the following Hamiltonian density [8]:

$$h(\mathbf{r}) = \begin{bmatrix} -iv\partial & T(\mathbf{r}) \\ T^{\dagger}(\mathbf{r}) & -iv\partial \end{bmatrix}, \quad T(\mathbf{r}) \equiv \begin{bmatrix} vV(\mathbf{r}) & uU^{*}(-\mathbf{r}) \\ uU(\mathbf{r}) & vV(\mathbf{r}) \end{bmatrix}, \quad (1)$$

where $-i\nu \partial$ is the Hamiltonian density for a single layer of graphene with $\emptyset \equiv \sigma^i \partial_i$, and $T(\mathbf{r})$ is the interlayer tunneling matrix and encodes the periodic profile of the moiré pattern, Fig. 4. $V(\mathbf{r}) = \sum_{j} e^{-i\mathbf{q}_{j}\cdot\mathbf{r}}$ takes the electron from one sublattice (either A or B) to the same sublattice on the other layer, while $U(\mathbf{r}) = \sum_{j} e^{-i\mathbf{q}_{j}\cdot\mathbf{r}} e^{i(j-1)2\pi/3}$ takes it to the opposing sublattice, with \vec{v} and \vec{u} being the corresponding tunneling amplitudes and j = 1, 2, 3. Note that L is the distance between neighboring AA and BB stackings in the moiré bilayer graphene, while the distance between two neighboring AA stackings is $\sqrt{3}L$ which therefore is also the periodicity of the Hamiltonian above; see Fig. 2.

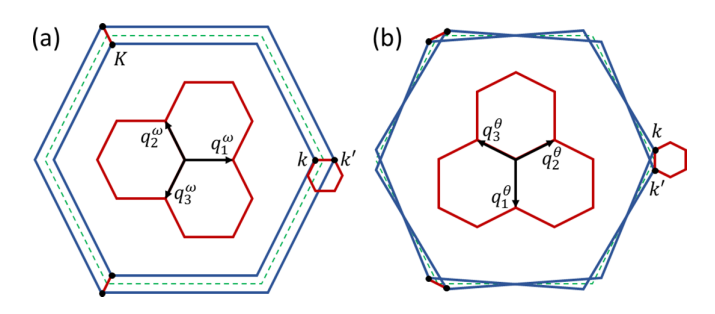


FIG. 1. Each blue hexagon designates the Brillouin zone of a single layer of graphene that has gone under either a strain, ξ_{ω} , or a twist, ξ_{θ} . In (a), the Brillouin zones are expanded/shrunken with respect to the undeformed Brillouin zone (green dotted hexagon), where as in (b), they are rotated with respect to each other. Each pair gives rise to its moiré reciprocal lattice (shown by red hexagonals). Also K points are designated by black dots.

Using the algebra of gamma matrices, $\{\gamma^{\mu}, \gamma^{\nu}\} = 2\eta^{\mu\nu}$, with $\eta_{\mu\nu}$ as the metric, and the unitary transformation,

$$h(\mathbf{r}) \to \Omega h(\mathbf{r})\Omega^{\dagger} \text{ with } \Omega = \frac{1}{\sqrt{2}} \begin{bmatrix} -1 & 1\\ \sigma^z & \sigma^z \end{bmatrix},$$
 (2)

we can write the Hamiltonian density (1) in terms of Dirac fermions coupled to nonfluctuating gauge fields as follows:

$$H = \int d^2x [\bar{\psi}i\nu\gamma^a(\partial_a + i\mathcal{A}_a\gamma_5 + i\mathcal{S}_ai\gamma_3)\psi - \bar{\psi}\gamma^0\mathcal{A}_0\gamma_5\psi - \bar{\psi}\gamma^0\mathcal{S}_0i\gamma_3\psi], \tag{3}$$

with $\bar{\psi} \equiv \psi^{\dagger} \gamma^0$. Or in the even tidier action formulation,

$$S = \int d^3x \, \bar{\psi} i \not\!\!D \psi, \quad \not\!\!D \equiv \gamma^{\mu} (\partial_{\mu} + i \mathcal{A}_{\mu} \gamma_5 + i \mathcal{S}_{\mu} i \gamma_3), \quad (4)$$

where a=1 and 2, $\mu=0$, 1, and 2, and the field components are

$$\mathcal{A}_{0} = -\frac{v}{v} \operatorname{Re}[V(\mathbf{r})], \quad \mathcal{S}_{0} = \frac{v}{v} \operatorname{Im}[V(\mathbf{r})],$$

$$\mathcal{A}_{1} = \frac{u}{2v} \operatorname{Re}[U(\mathbf{r}) + U(-\mathbf{r})], \quad \mathcal{A}_{2} = \frac{u}{2v} \operatorname{Im}[U(\mathbf{r}) + U(-\mathbf{r})],$$

$$\mathcal{S}_{1} = \frac{u}{2v} \operatorname{Im}[U(-\mathbf{r}) - U(\mathbf{r})], \quad \mathcal{S}_{2} = \frac{u}{2v} \operatorname{Re}[U(\mathbf{r}) - U(-\mathbf{r})].$$
(5)

The total field strength associated with D is given by $F_{\mu\nu}=\gamma_5 F_{\mu\nu}^{\mathcal{A}}+i\gamma_3 F_{\mu\nu}^{\mathcal{S}}+2i\gamma_5\gamma_3 \mathcal{A}_{\mu} S_{\nu}$, with $F_{\mu\nu}^{\mathcal{A},\mathcal{S}}$ being the field strengths generated by \mathcal{A}_{μ} and \mathcal{S}_{μ} , respectively.

Looking at the action (4), we see that the bilayer problem has transformed into that of Dirac fermions moving in a (2+1)-dimensional spacetime and acted upon by two axialvector fields: a chiral gauge field \mathcal{A}_{μ} and a spin field \mathcal{S}_{μ} . Note that γ_3 measures the spin along the direction normal to the material plane. The gauge fields, (5), are periodic with periodicity $\sqrt{3}L$, hence their corresponding field strengths are proportional to 1/L and also periodic with the same period, while the distance between each minimum and its neighboring maximum is L (see Fig. 3, for example). In particular, the spatial part of the field strength $F_{12}^{\mathcal{A}} = \partial_2 \mathcal{A}_1 - \partial_1 \mathcal{A}_2$ is

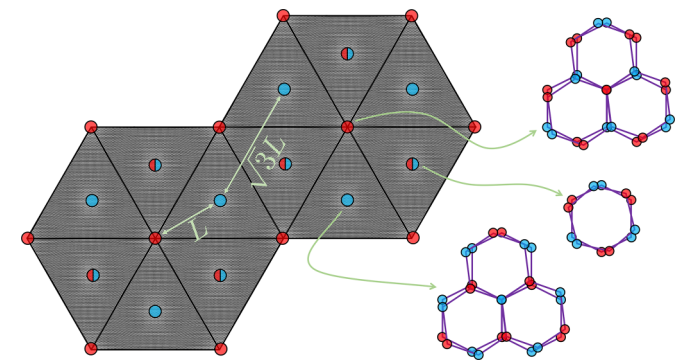


FIG. 2. Graphene has two sites, A and B, per unit cell. Where A sites of the layers exactly coincide we have AA stacking designated by red dots, while similarly BB stacking is designated by blue dots. Half red/blue dots show where the centers of the hexagons coincide in the bilayer. The distance between neighboring AA stackings is $\sqrt{3}L$.

given by

$$B(\mathbf{r}) \equiv F_{12}^{\mathcal{A}} = \frac{u}{v} \sum_{j} \hat{\mathbf{q}}_{j}^{\theta} \cdot \nabla(\mathbf{q}_{j} \cdot \mathbf{r}) \sin(\mathbf{q}_{j} \cdot \mathbf{r}), \quad (6)$$

where $\hat{\mathbf{q}}_{j}^{\theta} \cdot \nabla$ is the derivative along the unit vector $\hat{\mathbf{q}}_{j}^{\theta} \equiv \mathbf{q}_{j}^{\theta}/|q_{j}^{\theta}|$. That of \mathcal{S}_{a} equals $\frac{u}{v} \sum_{j} \hat{\mathbf{q}}_{j}^{\theta} \cdot \nabla(\mathbf{q}_{j} \cdot \mathbf{r}) \cos(\mathbf{q}_{j} \cdot \mathbf{r})$.

Consider the following chiral transformations associated with action (4):

with $\Gamma \equiv \gamma_0 \gamma_3 \gamma_5$. Each one of the above chiral transformations can become a symmetry of the action (4) under additional constraints: $\psi \to e^{i\alpha\gamma_5}\psi$, $\psi \to e^{i\alpha i\gamma_3}\psi$, and $\psi \to e^{i\alpha\Gamma}\psi$ are promoted to symmetries if $S_\mu = 0$, $A_\mu = 0$, and $A_0 = S_0 = 0$, respectively. Chiral particles can be defined with respect to each of these symmetries by using projection operators, e.g., $\psi_\pm \equiv \frac{1}{2}(1 \pm \gamma_5)\psi$. Since γ_5 and γ_3 do not commute we cannot simultaneously create fermions with definite γ_5 and γ_3 handedness, in contrast to Γ which commutes with both. So we can, for example, have $\psi_\uparrow^{\circlearrowleft,\circlearrowleft} \equiv \frac{1}{4}(1 \pm i\gamma_3)(1 \pm \Gamma)\psi$.

Our interest here is focused, more than anything else, on flat bands, which can be looked at as a class of modes covering the whole Brillouin zone at constant energy, $\bar{\psi}_k \gamma^0 \partial_0 \psi_k = \mu \psi_k^{\dagger} \psi_k$, within which the electrons are therefore localized $\partial E_k/\partial k = 0$. If we only consider this class, we eliminate the time dependence from the action entirely and reduce the (2+1)-dimensional theory to its (2+0)-dimensional version. Specifically, in the case of v=0, which supports exact flat bands [4], we have

$$I = \int \mathcal{D}\bar{\psi}\psi \exp\left\{\int d^2x \,\bar{\psi}i\gamma^a(\partial_a + i\mathcal{A}_a\gamma_5 + i\mathcal{S}_ai\gamma_3)\psi\right\}.$$
(8)

Using any of the chiral projections, $\psi_{\pm \text{ or } \uparrow\downarrow}^{\circlearrowleft,\circlearrowleft}$, we can break the above path integral further down, for instance, to

$$I = \int \mathcal{D}\bar{\psi}_{\pm}\psi_{\pm} \exp\left\{ \int d^{2}x [\bar{\psi}_{\pm}i\gamma^{a}(\partial_{a} \pm i\mathcal{A}_{a})\psi_{\pm} + \bar{\psi}_{\mp}\gamma^{a}\epsilon_{ab}\mathcal{S}^{b}\psi_{\pm}] \right\}, \tag{9}$$

where the path integral is over the four field variables $\bar{\psi}_{\pm}$ and ψ_{\pm} , while ψ_{\pm} fermions are coupled to $\pm A_a$.

In this form, the anomaly residing in the theory given by the path integral (8) takes the familiar shape of the chiral anomaly in two-dimensional Euclideanized space-time. In a path integral such as above, the gauge field A_a has an index associated with it that is directly given by the chiral anomaly [14–16]. However, the index must be an integer number which as we will see is only possible for certain values of θ and ω that coincide with the magic angle. This consistency condition can therefore tell us whether a flat band exists or not. Before proceeding to a more detailed investigation, it is worth mentioning that this reasoning, following the reduction from Eqs. (4) to (9), is generalizable to other perhaps more complicated systems such as multilayer graphene. In which case, we should use higher dimensional gamma matrices to accommodate for the additional layers. Other examples may include Refs. [17–19].

Since the gauge potentials are periodic the path integral can be divided into equivalent patches sewn together by an integration over all field configurations on the boundaries:

$$I = \int \prod_{\nabla} \mathcal{D}\bar{\psi}_{\partial\nabla} \psi_{\partial\nabla} I_{\nabla} [\bar{\psi}_{\partial\nabla}, \psi_{\partial\nabla}], \qquad (10)$$

with
$$I_{\nabla}[\bar{\psi}_{\partial\nabla}, \psi_{\partial\nabla}] = \int_{\bar{\psi}_{\partial\nabla}, \psi_{\partial\nabla}} \mathcal{D}\bar{\psi}_{\nabla}\psi_{\nabla}e^{iS_{\nabla}},$$
 (11)

where $\partial \nabla$ designates the boundary of the patches and the configuration residing on it, while ∇ designates the patch itself. In the first line, we are integrating over the boundary field configurations, $\int \prod_{\nabla} \mathcal{D}\bar{\psi}_{\partial\nabla}\psi_{\partial\nabla}$, while I_{∇} is the path integral over all configurations on one patch, $[\bar{\psi}_{\nabla}, \psi_{\nabla}]$, that end up as $[\bar{\psi}_{\partial\nabla}, \psi_{\partial\nabla}]$ on the boundary. Also S_{∇} is the same action before but with an integral only over ∇ . The patches are chosen so that the action S_{∇} is the same in all I_{∇} . While satisfying this property, we choose ∇ so that S_a will either vanish on or be perpendicular to $\partial \nabla$. Note that we can treat the theory represented as Eq. (9) as our starting point, forgetting where it came from, and then patch it up in any way we favor.

If the fermions remain confined within one patch, which should be the case when they are localized, we can exclude from the path-integration those configurations that connect different patches together. The probability density and current are here given by $\psi^{\dagger}\psi$ and $j^a \equiv \bar{\psi}\gamma^{\mu}\psi$, respectively. We expect the excluded configurations to be those with a nonzero flow of probability current, j^a , out of ∇ : $\int_{\nabla} \partial_0 \psi^{\dagger} \psi = \int_{\nabla} \partial_a j^a = \int_{\partial\nabla} \hat{n}^a_{\partial\nabla} \cdot j_a \neq 0$. In that case, the problem is reduced, from the initial path integral I, to segregated path

integrals of $I_{\nabla} = \int \mathcal{D}\bar{\psi}_{\nabla}\psi_{\nabla} \exp\{iS_{\nabla}\}$. If, moreover, there is a flat-band then the transition amplitude and thus the path integral, from any state to any other state within the band would be time independent

$$\langle \zeta | e^{iHt} | \chi \rangle \equiv \int_{\gamma}^{\zeta} \mathcal{D}\bar{\psi} \psi e^{iS} = \langle \zeta | \chi \rangle.$$
 (12)

This allows us to reduce the theory to (2 + 0) dimensions as in Eq. (4) to Eq. (9):

$$I_{\nabla} = \int_{\nabla} \mathcal{D}\bar{\psi}_{\pm}\psi_{\pm} \exp\left\{ \int_{\nabla} d^{2}x [\bar{\psi}_{\pm}i\gamma^{a}(\partial_{a} \pm i\mathcal{A}_{a})\psi_{\pm} + \bar{\psi}_{\mp}\gamma^{a}\epsilon_{ab}\mathcal{S}^{b}\psi_{\pm}] \right\}, \tag{13}$$

where we have removed the ∇ sign from the fermionic field variables (and brought it under the path integral sign instead) to avoid clutter. The most important role of the spin field S_a is that it takes ψ_{\pm} to ψ_{\mp} which is required for an intact patching of neighboring ∇ s [20]. Otherwise wave functions leak and the flat band gains a curvature. Effectively one can translate this into periodically changing the sign of the gauge field A_a so that its field strength will not average to zero. For the moment, we assume this role played and refer the reader to Ref. [21] for the detailed discussion.

Focusing only on I_{∇} , we see however, that not all gauge field configurations fit within the boundaries $\partial \nabla$; only those with a complete integer index, $n_{\circlearrowleft} - n_{\circlearrowleft} \in \mathbb{Z}$. One way to observe this is first to notice that a continuous chiral rotation of $\psi_+ \to e^{i2\pi\Gamma}\psi_+ = \psi_+$ takes the spinor field to itself while leaving the action unchanged. However, the theory (13) is subject to chiral anomaly, namely, the Jacobian of our chiral transformation, J_5 , is nontrivial,

$$I_{\nabla} = \int_{\nabla} [\mathcal{D}\bar{\psi}_{+}\psi_{+}] \mathcal{D}\bar{\psi}_{-}\psi_{-}e^{iS_{\nabla}}$$

$$\longrightarrow \int_{\nabla} [\mathcal{D}\bar{\psi}_{+}\psi_{+}J_{5}] \mathcal{D}\bar{\psi}_{-}\psi_{-}e^{iS_{\nabla}} = I_{\nabla}e^{i2\pi(n_{\bigcirc}-n_{\bigcirc})}.$$

$$(14)$$

The last equality above comes from knowing that the Jacobian of chiral transformation is connected to the Atiyah-Singer index [14,15,22]. Chiral transformation discriminates between right and left handed modes, $n_{\odot} - n_{\odot}$, hence the path integral (which yields the determinant of the Dirac operator) obtains a phase associated with this difference. This phase encodes the winding number of the gauge field associated with the Dirac operator—an integer number which in our two-dimensional system is written as

$$\frac{1}{2\pi} \int_{\nabla} d^2x \, \epsilon^{ab} \partial_a \mathcal{A}_b = n_{\circlearrowleft} - n_{\circlearrowleft} \,. \tag{15}$$

However, since the field variables do not change by a complete rotation, in Eq. (14), the path integral must also remain the same: $I_{\nabla} = I_{\nabla} e^{i2\pi(n_{\bigcirc} - n_{\bigcirc})}$. Thus, if $e^{i2\pi(n_{\bigcirc} - n_{\bigcirc})} \neq 1$, then the only way that the initial and the transformed path integrals can be equal is for them to vanish, $I_{\nabla} = 0$. This zero valued partition function means that the state is unrealizable.²

¹This way the edge configurations along $\partial \nabla$ will have an additional chiral symmetry with respect to $e^{i\alpha\gamma_5}$.

²In contrast, the flat-band can be realized if $n_{\circlearrowright,\circlearrowleft} \in \mathbb{Z}$.

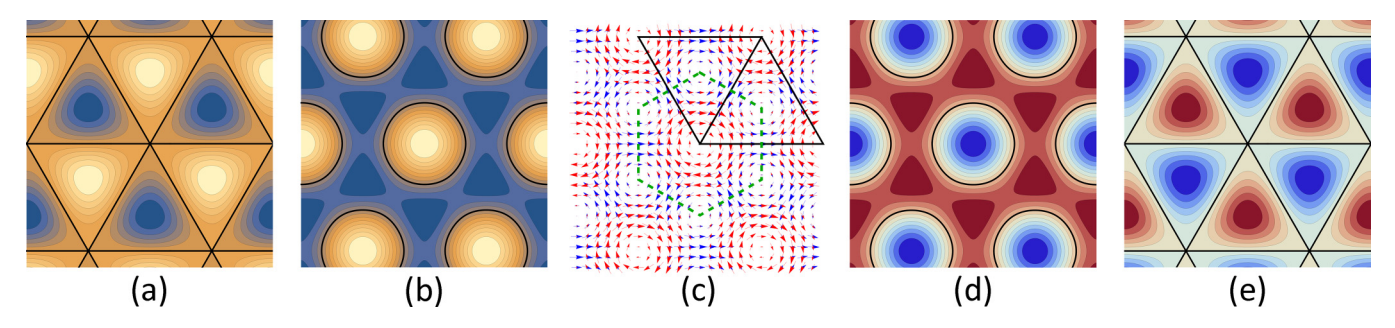


FIG. 3. (a) The magnetic field B created by A_a felt by ψ_+ while its negative is exerted upon the ψ_- . (b) The field strength associated with the spin field. (c) Vector fields A_a (blue) and S_a (red). The black line designates two magnetic regions related by parity. Parallel sides are identified with each other and the whole system can be reconstructed by sewing these together. The S_a field is zero everywhere on the green dashed hexagon. (d) The chiral scalar potential A_0 as experienced by ψ_+ and (e) that of S_0 . Except for (c) the fields are zero on the black curves. Note how S_0 coincides with the magnetic field in (a) and also how A_0 coincides with field strength in (b), in particular S_0 vanishes on edge of each magnetic region. Also note that a fermion configuration localized on the edge of each magnetic region will be perpendicular to S_a [see (c), for example].

What we have discussed so far applies generally to all deformations of any bilayer system that shares the symmetries of graphene. Let us now focus on uniform twist for which $\mathbf{q}_1 = \mathbf{q}^\theta = q^\theta(-1,0)$ and $\mathbf{q}_{2,3} = \mathbf{q}^\theta_{2,3} = q^\theta(\pm\sqrt{3}/2,1/2)$ with $q^\theta = 2K_D\sin(\theta/2) = 4\pi/3L$. The gauge fields \mathcal{A}_a and \mathcal{S}_a generated by uniform twist are divergenceless with their corresponding field strengths proportional to $u/\nu L$. These are depicted in Fig. 3. We need to calculate the minimum value of L corresponding to $n_0 = 1$. We find

$$n_{\odot} = \frac{1}{4\pi} \int_{\nabla} d^2x \, \epsilon^{ab} \partial_a A_b = \frac{1}{4\pi} \int_{\nabla} d^2x \, B = \frac{3\sqrt{3}u}{4\pi \nu} L \,, \quad (16)$$

which is equal to 1 for $L = L_0 \equiv 4\pi v/3\sqrt{3}u$. Considering $L = a/2\sin(\theta/2)$, where a = 2.46 Å is the graphene lattice constant, the first magic angle is given by $\theta \approx 3\sqrt{3}au/4\pi v \approx 1.1^{\circ}$ with u = 0.11 eV and $vK_D = 9.9$ eV.

To develop semiclassical intuition, let us first assume that the spin current term $S_a \bar{\psi} \gamma^a \gamma_3 \psi$ is disregardable. Then we are left with only a magnetic field with strength proportional

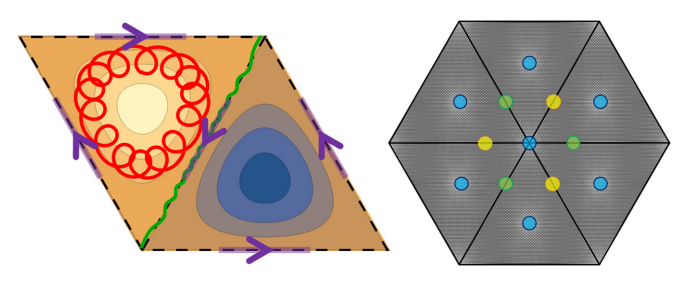


FIG. 4. On the left, a generic electron (red trajectory) drifting in the magnetic region while another electron (green trajectory) is moving close to the edge of one magnetic region. A right or left handed fermion belongs only to either of the magnetic regions but since the sides are identified a right handed fermion in one region is the left handed fermion in the other. Having one electron in both regions is similar to having two electrons in one region and forgetting about the other. On the right the twisted bilayer graphene at first magic angle with blue dots denoting AA stacking and yellow/green dots AB/BA stacking. The distance between the neighboring equivalent dots is equal to L.

to u/vL acting with opposite signs on ψ_{\pm} fermions that are completely decoupled from each other. If the magnetic field was constant across the material then the electrons would have been subject to Landau localization rotating around a fixed center, in a semiclassical picture, and forming Landau levels. Since the moiré effective magnetic field is inhomogeneous, the semiclassical picture changes to that of drifting fermions—rotating around a cycling center. See Fig. 4. For localization to be possible, the drifting fermion should be able to fit into one magnetic region. The smallest rotating fermion, according to the uncertainty principle, has a size of $\ell_B \propto 1/\sqrt{\bar{B}}$ and, since here the average magnetic field \bar{B} is proportional to 1/L, it expands with \sqrt{L} . However, the size of the magnetic regions, or ∇ , is proportional to L which grows faster than $\ell_B \propto \sqrt{L}$. Thus ∇ gets bigger faster than the smallest possible electron and eventually can catch one, at which moment one electron has just been trapped inside the magnetic region and can complete a cycle there without getting out of it.

At that moment, we expect to have an edge mode on the boundary of the magnetic region. Appropriately, for this mode the effect of spin current term on the magic angle is indeed disregardable since S_a and $\bar{\psi}\gamma^a\gamma_3\psi$ are perpendicular to each other on $\partial\nabla$. However, if there is an edge mode it means that the number of right- or left-handed fermions that reside in the magnetic region must at least be one, $n_{\circlearrowright,\circlearrowleft} = 1$. This again leads us to Eq. (16) and the magic angle. It also can be seen in terms of unit of flux and a restricted type of Landau quantization. For large $n \in \mathbb{Z}$ with $\ell_B = \sqrt{L\nu/u}$, we have $n = L^2/2\pi\ell_B^2 = uL/2\pi\nu$ as the degeneracy of the moiré Landau level. Thus we expect a series of magic angles connected to each other by steps of $\delta L \approx 2\pi\nu/u$.

The negligibility of S_a for the first magic angle suggests that the non-Abelian theory can be *Abelianized* for this case. For a similar process see Ref. [23] where a spin field, S_{μ} , is decoupled from the fermions. In turn, it means that the physics of the first magic angle maps to that of the lowest

³In terms of the parameter α introduced in Ref. [4], these are steps of $\delta\alpha \approx 3/2$ while the first magic angle corresponds to $\alpha \approx 1/\sqrt{3}$.

Landau level. For higher magic angles, as the zero-mode wave-functions become more complicated, the effects of S_a also become considerable. Since the field strength is given by $F_{\mu\nu} = \gamma_5 F_{\mu\nu}^A + i\gamma_3 F_{\mu\nu}^S + 2i\gamma_5\gamma_3 \mathcal{A}_\mu S_\nu$, the phase associated to non-Abelian part grows with L^2 while that of the Abelian part grows with L. Hence, Abelianization is plausible for $L \lesssim 4\pi \nu/3u$. For a longer discussion including the definition of Abelianization and few implications such as the first order correction due to S_a , see Ref. [21]. More detailed considerations are provided in a recent work Ref. [20]. Also look at Ref. [24] for a general discussion.

Reformulating the theory in terms of Dirac fermions (4) has extra merits. For example, the application of an external electromagnetic field yields the same theory (4) but now with the Dirac operator carrying an additional external gauge field, $A_{\mu\nu}$,

$$\not\!\!\!D \equiv \gamma^{\mu}(\partial_{\mu} + iA_{\mu} + iA_{\mu}\gamma_{5} + iS_{\mu}i\gamma_{3}).$$

Upon projecting the Dirac fermions into $\psi_{\pm} \equiv \frac{1}{2}(1 \pm \gamma_5)\psi$ as before, we see that the chiral fermions are now coupled to the shifted gauge fields $A_a \pm A_a$. For example, if A_a is due to a constant magnetic field H, Eq. (16) reads

$$n_{\odot} = \frac{1}{4\pi} \int_{\nabla} d^2x \, (H \pm B) = \frac{H}{4\pi} \frac{3\sqrt{3}}{4} L^2 \pm \frac{3\sqrt{3}u}{4\pi v} L \,.$$
 (17)

For $u^2/v^2 > 4\pi H/3\sqrt{3}$, the requirement $n_{\circlearrowright} = \pm 1$ has more than one solution in contrast to Eq. (16). Thus an external magnetic field splits each magic angle into

$$L = \pm \frac{u}{v} \frac{2}{H} \pm \sqrt{\left(\frac{u}{v} \frac{2}{H}\right)^2 \pm \frac{16\pi}{3\sqrt{3}H}},$$
 (18)

with the magic *angles* given by $\theta = 2\arcsin(a/2L)$, while each combination of pluses and minuses above yields a solution to Eq. (17). For a small external magnetic field $H \ll (3\sqrt{3}/4\pi)u^2/v^2 \approx 140$ mT, the positive solutions can

be written as

$$L_1^{\pm} = L_0 \pm \frac{4\pi^2}{27} \frac{v^3}{u^3} H, \quad L_2^{\pm} = \frac{4}{H} \frac{u}{v} \pm L_0 - \frac{4\pi^2}{27} \frac{v^3}{u^3} H.$$
 (19)

with $L_0 \equiv 4\pi v/3\sqrt{3}u$, being the magic angle in the absence of the external magnetic field. In the limit $H \to 0$, we regain the previous magic angle from L_1^{\pm} , in addition to having $L_2^{\pm} \to \infty$ that happens when the bilayer is untwisted, $\theta \to 0$, and the moiré reciprocal lattice, which would have a vanishing size, is in fact flat. The dispersion at this instance is that of two quadratic bands touching at the K point; or in other words a vanishing Dirac velocity. For a brief discussion about introducing strain and nonchiral components see Ref. [21].

As we have seen in this Letter, although anomalies are not present in all dimensions, it is still possible to conjure them in specific situations. In particular, a flat band can be described through an anomaly in the timeless version of its hosting theory. We saw that the dimensionally reduced theory and thus the flat band are not always realizable. In the case of bilayer graphene, the obstruction comes from the chiral anomaly and the need to satisfy an index condition, which in turn confirms the topological nature of the flat band. The Dirac field theory form, Eq. (4), of the bilayer moiré lattice problem allows many generalizations including the finite temperature case, the presence of complex inhomogeneous external fields and general deformations, and interaction effects in the spirit of Refs. [23,25,26] where the interplay of anomaly with interactions are discussed. Of particular interest are quantum Hall phenomena and unconventional superconducting pairing associated with the moiré gauge fields [24].

Note added. Recently, preprint [27] was posted with an alternative procedure for the Abelianization of the first magic angle.

This work was supported by the National Science Foundation under Grant No. DMR-2037158, the U.S. Army Research Office under Contract No. W911NF1310172, and the Simons Foundation.

^[1] J. M. B. Lopes dos Santos, N. M. R. Peres, and A. H. Castro Neto, Graphene bilayer with a twist: Electronic structure, Phys. Rev. Lett. 99, 256802 (2007).

^[2] R. Bistritzer and A. H. MacDonald, Moiré bands in twisted double-layer graphene, Proc. Natl. Acad. Sci. USA 108, 12233 (2011).

^[3] P. San-Jose, J. González, and F. Guinea, Non-Abelian gauge potentials in graphene bilayers, Phys. Rev. Lett. 108, 216802 (2012).

^[4] G. Tarnopolsky, A. J. Kruchkov, and A. Vishwanath, Origin of magic angles in twisted bilayer graphene, Phys. Rev. Lett. 122, 106405 (2019).

^[5] Y. Cao, V. Fatemi, S. Fang, K. Watanabe, T. Taniguchi, E. Kaxiras, and P. Jarillo-Herrero, Unconventional superconductivity in magic-angle graphene superlattices, Nature (London) 556, 43 (2018).

^[6] Y. Cao, V. Fatemi, A. Demir, S. Fang, S. L. Tomarken, J. Y. Luo, J. D. Sanchez-Yamagishi, K. Watanabe, T. Taniguchi, E.

Kaxiras *et al.*, Correlated insulator behaviour at half-filling in magic-angle graphene superlattices, Nature (London) **556**, 80 (2018).

^[7] E. Y. Andrei and A. H. MacDonald, Graphene bilayers with a twist, Nat. Mater. 19, 1265 (2020).

^[8] L. Balents, General continuum model for twisted bilayer graphene and arbitrary smooth deformations, SciPost Phys. 7, 048 (2019).

^[9] A. O. Sboychakov, A. L. Rakhmanov, A. V. Rozhkov, and F. Nori, Electronic spectrum of twisted bilayer graphene, Phys. Rev. B 92, 075402 (2015).

^[10] L. Zou, H. C. Po, A. Vishwanath, and T. Senthil, Band structure of twisted bilayer graphene: Emergent symmetries, commensurate approximants, and Wannier obstructions, Phys. Rev. B 98, 085435 (2018).

^[11] J. Liu, J. Liu, and X. Dai, Pseudo Landau level representation of twisted bilayer graphene: Band topology and implications on the correlated insulating phase, Phys. Rev. B **99**, 155415 (2019).

- [12] A. Parhizkar and V. Galitski, Strained bilayer graphene, emergent energy scales, and moiré gravity, Phys. Rev. Res. 4, L022027 (2022).
- [13] A. Parhizkar and V. Galitski, Moiré gravity and cosmology, arXiv:2204.06574.
- [14] K. Fujikawa and H. Suzuki, Path Integrals and Quantum Anomalies (Oxford University Press, Oxford, UK, 2004).
- [15] M. F. Atiyah and I. M. Singer, The index of elliptic operators on compact manifolds, Bull. Am. Math. Soc. 69, 422 (1963).
- [16] A complete consideration must take the non-Abelian chiral anomaly into account.
- [17] N. Paul, Y. Zhang, and L. Fu, Giant proximity exchange and flat chern band in 2D magnet-semiconductor heterostructures, Sci. Adv. 9, eabn1401 (2023).
- [18] J. Dong, J. Wang, and L. Fu, Dirac electron under periodic magnetic field: Platform for fractional Chern insulator and generalized Wigner crystal, arXiv:2208.10516.
- [19] Y.-Z. Chou, Y. Fu, J. H. Wilson, E. J. König, and J. H. Pixley, Magic-angle semimetals with chiral symmetry, Phys. Rev. B 101, 235121 (2020).

- [20] A. Parhizkar and V. Galitski, Zero flux localization: Magic revealed, arXiv:2409.05942.
- [21] See Supplemental Material at http://link.aps.org/supplemental/ 10.1103/PhysRevB.110.L121111 for the introduction of the Abelianization process and the modifications due to strain.
- [22] K. Fujikawa, Path-integral measure for gauge-invariant fermion theories, Phys. Rev. Lett. 42, 1195 (1979).
- [23] C. Rylands, A. Parhizkar, and V. Galitski, Non-Abelian bosonization in a (3 + 1)-d Kondo semimetal via quantum anomalies, Phys. Rev. B **105**, 195108 (2022).
- [24] A. Parhizkar and V. Galitski, Localizing transitions via interaction-induced flat bands, arXiv:2308.16440.
- [25] C. Rylands, A. Parhizkar, A. A. Burkov, and V. Galitski, Chiral anomaly in interacting condensed matter systems, Phys. Rev. Lett. 126, 185303 (2021).
- [26] A. Parhizkar, C. Rylands, and V. Galitski, Path integral approach to quantum anomalies in interacting models, Phys. Rev. B 109, 155109 (2024).
- [27] V. Crépel, P. Ding, N. Verma, N. Regnault, and R. Queiroz, Topologically protected flatness in chiral moiré heterostructures, arXiv:2403.19656.